NUREG/CR–6851
ANL-04/14

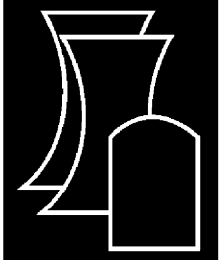

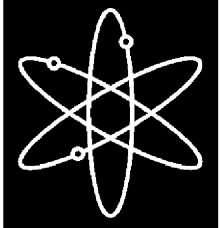

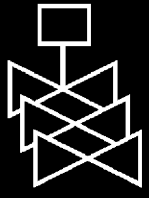

Hydrogen Effects on Air Oxidation of Zirlo Alloy

Argonne National Laboratory

U.S. Nuclear Regulatory Commission
Office of Nuclear Regulatory Research
Washington, DC 20555-0001

AVAILABILITY OF REFERENCE MATERIALS IN NRC PUBLICATIONS

NRC Reference Material

As of November 1999, you may electronically access NUREG-series publications and other NRC records at NRC's Public Electronic Reading Room at http://www.nrc.gov/reading-rm.html. Publicly released records include, to name a few, NUREG-series publications; *Federal Register* notices; applicant, licensee, and vendor documents and correspondence; NRC correspondence and internal memoranda; bulletins and information notices; inspection and investigative reports; licensee event reports; and Commission papers and their attachments.

NRC publications in the NUREG series, NRC regulations, and *Title 10, Energy*, in the Code of *Federal Regulations* may also be purchased from one of these two sources.

1. The Superintendent of Documents
   U.S. Government Printing Office
   Mail Stop SSOP
   Washington, DC 20402–0001
   Internet: bookstore.gpo.gov
   Telephone: 202-512-1800
   Fax: 202-512-2250
2. The National Technical Information Service
   Springfield, VA 22161–0002
   www.ntis.gov
   1–800–553–6847 or, locally, 703–605–6000

A single copy of each NRC draft report for comment is available free, to the extent of supply, upon written request as follows:

Address: Office of the Chief Information Officer,
Reproduction and Distribution
Services Section
U.S. Nuclear Regulatory Commission
Washington, DC 20555-0001
E-mail: DISTRIBUTION@nrc.gov
Facsimile: 301–415–2289

Some publications in the NUREG series that are posted at NRC's Web site address http://www.nrc.gov/reading-rm/doc-collections/nuregs are updated periodically and may differ from the last printed version. Although references to material found on a Web site bear the date the material was accessed, the material available on the date cited may subsequently be removed from the site.

Non-NRC Reference Material

Documents available from public and special technical libraries include all open literature items, such as books, journal articles, and transactions, *Federal Register* notices, Federal and State legislation, and congressional reports. Such documents as theses, dissertations, foreign reports and translations, and non-NRC conference proceedings may be purchased from their sponsoring organization.

Copies of industry codes and standards used in a substantive manner in the NRC regulatory process are maintained at—

The NRC Technical Library
Two White Flint North
11545 Rockville Pike
Rockville, MD 20852–2738

These standards are available in the library for reference use by the public. Codes and standards are usually copyrighted and may be purchased from the originating organization or, if they are American National Standards, from—

American National Standards Institute
11 West 42nd Street
New York, NY 10036–8002
www.ansi.org
212–642–4900

Legally binding regulatory requirements are stated only in laws; NRC regulations; licenses, including technical specifications; or orders, not in NUREG-series publications. The views expressed in contractor-prepared publications in this series are not necessarily those of the NRC.

The NUREG series comprises (1) technical and administrative reports and books prepared by the staff (NUREG–XXXX) or agency contractors (NUREG/CR–XXXX), (2) proceedings of conferences (NUREG/CP–XXXX), (3) reports resulting from international agreements (NUREG/IA–XXXX), (4) brochures (NUREG/BR–XXXX), and (5) compilations of legal decisions and orders of the Commission and Atomic and Safety Licensing Boards and of Directors' decisions under Section 2.206 of NRC's regulations (NUREG–0750).

NUREG/CR-6851
ANL-04/14

Hydrogen Effects on Air Oxidation of Zirlo Alloy

Manuscript Completed: August 2004
Date Published: October 2004

Prepared by
K. Natesan, W.K. Soppet

Argonne National Laboratory
9700 South Cass Avenue
Argonne, IL 60439

S. Basu, NRC Project Manager

Prepared for
Division of Sytems Analysis and Regulatory Effectiveness
Office of Nuclear Regulatory Research
U.S. Nuclear Regulatory Commission
Washington, DC 20555-0001
NRC Job Code Y6512

Hydrogen Effects on Air Oxidation of Zirlo Alloy

by

K. Natesan and W. K. Soppet

Abstract

An experimental program was conducted to generate data on the air oxidation kinetics of unirradiated Zirlo cladding with preoxidation and prehydriding to simulate inventory of spent fuel discharge after a medium or high level of fuel burnup. The oxide layer on the cladding was formed by a preoxidation step in a steam environment for 140 h at 550°C, which resulted in an oxide thickness in the range of 25-30 μm. Prehydriding treatment was done by charging hydrogen to cladding and the process was tailored to produce hydrogen concentration in the range of 100-1000 wppm, typical of medium to high burnup cladding. The prehydrided and prehydrided/steam-preoxidized specimens were subsequently oxidized in air at temperatures in the range of 300-600°C. The maximum air oxidation times ranged between 300 h at 600°C and ≈1000 h at 300°C. Weight-change and oxide-thickness were measured on the specimens exposed at various times to establish the kinetics of the scaling process as a function of temperature. Extensive metallography and hardness measurements were performed on the tested specimens to examine the oxide scale development and hydrogen ingress into the material. Weight-change and oxide-thickness data, generated in the present program, were used to develop correlations to depict the air oxidation behavior of prehydrided alloys with and without steam preoxidation. A comparison of the oxidation data on Zirlo with and without prehydriding (performed in gas phase hydrogen and/or in steam) indicated that hydrogen concentration in the range of 100-1000 wppm had minimal effect on the Zirlo oxidation rate in air at temperatures in the range of 300-600°C.

Contents

Figures

Tables

Executive Summary

The kinetics of cladding oxidation in an air environment is important in many safety-related studies on nuclear reactors. For example, in a pressurized thermal shock event, the reactor pressure vessel may be breached, leading to air intrusion in the core and consequent oxidation of relatively cold fuel cladding. Another example is structural failure of the dry storage and transportation cask, which may result in air intrusion and consequent interaction with the spent fuel rods. In spent fuel pool accidents arising from loss of pool inventory, spent fuel rods can be exposed to an air environment. In all these cases, knowledge of the air oxidation kinetics of the cladding at relatively low temperatures is essential in assessing and determining the margin for its integrity.

In an extensive experimental study, we previously tested Zircaloy-4, Zirlo, and M5 cladding materials to establish the air oxidation kinetics for the alloys in both bare and steam-preoxidized conditions (Natesan and Soppet, 2004). Weight change and oxide thickness were measured over a wide temperature range, and the results from that study were used to develop oxidation rate correlations for all three materials. The study showed that all three alloys, initially in the steam-preoxidized condition, could undergo further oxidation in the event of air ingress. It was concluded that the rate at which the oxide scale grows is dependent on the cladding temperature, exposure time, and alloy composition. The data and correlations on oxide scale development were presented in an earlier report (NUREG/CR-6846).

The objective of this program is to obtain experimental data on the air oxidation kinetics of unirradiated Zirlo cladding that has been prehydrided in hydrogen gas with or without steam preoxidation. Experiments were conducted in which Zirlo ring and capsule specimens were exposed in a hydrogen environment at 320°C and for various time periods. Prehydriding treatment was tailored to obtain hydrogen concentrations in a range of 100-1000 wppm. Steam preoxidation treatment was conducted to obtain an oxide thickness of ≈25 μm. The prehydrided and prehydrided/steam-preoxidized Zirlo capsule specimens were subsequently oxidized in air at temperatures in the range of 300-600°C. The maximum air oxidation times ranged between ≈1000 h at 300°C and 300 h at 600°C. Weight change and oxide thickness were measured on the specimens exposed at various times to establish the kinetics of the scaling process as a function of temperature.

Extensive metallography of cross sections of prehydrided and air-oxidized specimens was conducted to measure the scale thickness and to establish the distribution of hydride precipitates across the cladding thickness. Hardness measurements were made on specimens with various treatments to examine the variation, if any, in the strength of the alloy due to hydrogen ingress. Knoop hardness indentations that were made at several locations across the cladding thickness in various specimens exhibited negligible variation, indicating uniform distribution of hydrogen.

The air-oxidized specimens with various pretreatments were analyzed for hydrogen content, and the results were used to correlate the parabolic oxidation rate and oxide-thickness growth rate with hydrogen concentration in the alloy. Data indicated that exposure of the Zirlo specimen at elevated temperature (e.g., steam preoxidation at 550°C) had a much more softening effect than the hardening effect that can result from higher hydrogen content (e.g., 695 and 735 wppm in steam oxidized specimens).

We concluded that hydrogen concentration in Zirlo in the range of 100-1000 wppm has negligible deleterious effect on the kinetics of oxidation in air at temperatures in the range of 300-600°C. Furthermore, the scaling data indicated a negligible effect of hydrogen concentration in the range of 100-1000 wppm on the scale growth.

Foreword

The kinetics of cladding oxidation in air environment is important in many safety-related investigations. For example, in spent fuel pool accident arising from loss of pool water inventory, spent fuel rods can be exposed to an air environment. Knowledge of air oxidation kinetics of cladding at relatively low temperatures is needed in assessing safety and determining the margin for clad integrity in all these cases. Prior data on cladding oxidation in air environment was based on a very limited set of experiments not directly applicable to the low temperature range of interest for the above cases. More recently, a research program, sponsored by the NRC Office of Nuclear Regulatory Research was conducted at the Argonne National Laboratory to obtain experimental data on air oxidation kinetics of cladding which are representatives of current and/or projected inventory in operating reactors and in spent fuel discharged after a medium or high level of fuel burnup. The program consisted of a large number of experiments with specimens of Zircaloy-4, Zirlo, and M5 cladding in which the specimens were subjected to isothermal air oxidation at different temperatures and for different duration of time. The specimens were unirradiated but simulated in-reactor conditions in terms of oxide growth. Results from these experiments, documented previously in a report (NUREG/CR-6846) published in June 2004, indicated no discernible deleterious effect of the pre-existing oxide layer from the in-reactor operation on further clad oxidation in an air environment. The results also confirmed that the correlations developed in this experimental study are in fair agreement with those used previously for the spent fuel pool risk study.

The present report documents the results of additional experiments conducted at the Argonne National Laboratory to investigate the effect of hydrides on subsequent air oxidation kinetics of cladding. The hydrides form on the cladding surface during in-reactor operation as a result of hydrogen pickup from the corrosion process during oxidation of cladding by water and steam. The hydrogen picked up migrates in colder regions of the cladding and tends to form hydride rings or pockets of concentrated hydrides. The hydrides have potential deleterious effects on subsequent oxidation kinetics and mechanical behavior of the cladding. The additional experiments were performed with Zirlo cladding which comprises, in large part, the inventory of most recently discharged fuel in spent fuel pool, particularly that related to higher burnup fuel. The older fuels have Zircaloy-4 cladding, which is known to pick up substantially more hydrogen than Zirlo at a higher burnup. However, these fuels have much less decay heat associated with them and, as such, the cladding is not prone to significant thermal stress or accelerated oxidation kinetics. In contrast to Zircaloy-4 and Zirlo, there is very little, if any, current or projected inventory of M5 cladding in the spent fuel pool. Besides, the M5 cladding is known to pick up less hydrogen during in-reactor operation compared to Zirlo and Zircaloy-4 and, as such, the effect of hydrides may be less significant for M5.

The results of the current series of experiments show that hydrogen pickup in Zirlo in the range of 100-1000 wppm during in-reactor operation has negligible effect on the kinetics of oxidation in air at temperatures in the range of 300-600°C. Noting that this level of hydrogen pickup is representative of medium to high burnup operation, the results suggest no noticeable deleterious effect of hydrides on air oxidation of Zirlo that was previously oxidized in steam environment during in-reactor operation. At temperatures higher than 600°C, the hydrides go into solution and do not affect the cladding behavior and thus, the air oxidation kinetics. The air oxidation data reported here and in the companion report NUREG/CR-6846 will provide more

realistic analysis of the spent fuel pool heatup and thus will add more confidence on the analysis of spent fuel pool safety issues.

Farouk Eltawila, Director
Division of Systems Analysis and Regulatory Effectiveness

Acknowledgments

This work is sponsored by the Office of Nuclear Regulatory Research, U.S. Nuclear Regulatory Commission, under Job Code Y6512; Program Manager: S. Basu. Cladding tubes of Zirlo were supplied by Westinghouse, Pittsburgh, PA. L. Cairo and M. Baquera assisted in the metallography and in oxide thickness and hardness measurements of the hydrogen-charged and air-oxidized specimens. Hydrogen, oxygen, and nitrogen analyses were performed by Argonne National Laboratory, LECO Corporation, and Staveley Company.

1 Introduction

The kinetics of cladding oxidation in an air environment is important in many safety-related studies on nuclear reactors. For example, in a pressurized thermal shock event, the reactor pressure vessel may be breached, leading to air intrusion in the core and consequent oxidation of relatively cold fuel cladding. Another example is structural failure of the dry storage and transportation cask, which may result in air intrusion and consequent interaction with the spent fuel rods. In both cases, knowledge of the air oxidation kinetics of the cladding at relatively low temperatures is essential in assessing and determining the margin for its integrity.

Zirconium-based alloys are prone to oxidize fairly easily because of their affinity for oxygen and the inherent thermodynamic stability of the zirconium oxide that forms when the alloys are exposed to steam and air environments at elevated temperatures. High temperature oxidation of zirconium and zirconium alloys in oxygen, air, and steam has been the subject of extensive research due to their use as cladding materials in nuclear reactors (Cubiciotti, 1950; Gulbransen and Andrew, 1957; Pemsler, 1962, 1964; Mackay, 1963; Wallwork et al., 1964; Kidson, 1966; Com-Nougue et al., 1969; Pawel, 1979; Pawel and Campbell, 1980). Over the years, several studies have been conducted to evaluate the kinetics of oxidation of Zr-based alloys in steam environments, but most of the studies were conducted at temperatures >700°C on bare alloys and for short time periods to predict the cladding behavior under loss-of-coolant situations (Leistikow et al., 1978, 1980; Leistikow and Berg, 1987; Moalem and Olander, 1991; Rosa and Smeltzer, 1980; Powers et al., 1994). The effect of hydrogen, if any, on the oxidation process was not evaluated in these studies.

During the past two years, an extensive oxidation study was conducted at Argonne National Laboratory on Zr-based cladding materials to establish the air oxidation kinetics for the alloys in both bare and steam-preoxidized conditions (Natesan and Soppet, 2004). The objective of the program was to obtain experimental data on the air oxidation kinetics of unirradiated Zircaloy-4, Zirlo, and M5 cladding with an oxide layer that is representative of the current inventory of spent fuel discharged after a medium or high level of fuel burnup. Weight change and oxide thickness were determined for bare and steam preoxidized conditions over a wide temperature range, and the results were used to develop oxidation rate correlations for all three materials.

The expected oxide thickness on the cladding stored in spent fuel pool is in the range of 25-30 μm after service in medium burnup conditions and can be as high as 100 μm after high burnup service. The aim of the earlier study was to preoxidize the bare cladding in a steam environment to achieve an oxide thickness of 25-30 μm, which simulates the oxide layer on the cladding in spent fuel pool (Natesan and Soppet, 2004). The air oxidation tests were performed on the steam-preoxidized cladding at temperatures representative of cladding heatup in the event of a partial or full draining of spent fuel pool coolant. Tests were performed on all three alloys over a wide temperature range of 300-900°C, with emphasis on the low temperature regime of 300-600°C.

The present study aims to examine the role, if any, of hydrogen ingress into the alloy on subsequent oxidation of Zirlo cladding in an air environment. The report discusses the hydrogen uptake by Zirlo in a gaseous hydrogen and a steam environment. Experimental procedures are described and kinetic data are presented on air oxidation of prehydrided and prehydrided/steam-preoxidized Zirlo alloy in both ring and capsule forms at temperatures in the

range of 300-600°C. Hydrogen concentration in the specimens in the prehydrided condition was confined to a range of 100-1000 wppm. Extensive metallography of cross sections of prehydrided and air-oxidized specimens was conducted to measure the scale thickness and to establish the distribution of hydride precipitates across the cladding thickness. Hardness measurements were made on specimens with various treatments to examine the indentation size, and thereby establish the hydrogen distribution across the thickness of the cladding. The air-oxidized specimens with various pretreatments were analyzed for hydrogen content, and the results were used to correlate the parabolic oxidation rate and oxide-thickness growth rate with hydrogen concentration in the alloy.

2 Background

Zirconium-based alloys, in general, have a strong affinity for oxygen, nitrogen, and hydrogen, and the cladding, such as Zirlo, could develop a zirconium oxide (ZrO_2) scale during reactor service, as a result of chemical reaction of Zr metal with water. At the same time, the alloy also absorbs hydrogen, that is released from reaction of the Zr metal with water. The thickness of the external oxide scale and amount of hydrogen ingress into the alloy are strongly dependent on exposure time and temperature. Figure 2.1 shows the Zr-H phase diagram, indicating a low solubility value for hydrogen in the alloy (α phase) at the reactor operating temperature of 320°C (Hansen and Anderko, 1958).

Several investigators have measured the solubility of hydrogen in Zr-based alloys by a variety of techniques (Gulbransen and Andrew, 1955; Sawatzky, 1960; Ostberg, 1962; Westerman, 1966; Erickson and Hardie, 1964; and Kearns, 1967). Several studies concluded that Zr and its alloys exhibit significant supersaturation of hydrogen, depending on the alloy composition. As a result, there was significant scatter in the solubility values measured by different investigators. Kearns (1967) measured solubility by a diffusion couple method, which was not subject to supersaturation. To check possible compositional effects, he used iodide and sponge zirconium, Zircaloy-2, and Zircaloy-4.

Kearns determined the terminal solubility by hydrogen analysis of the low-hydrogen part of diffusion couples made by resistance welding hydride-bearing samples (2.5-cm long) to opposite sides of hydrogen-free samples (0.64-cm long) and annealing to equilibrium in the temperature range of 260 to 525°C. The hydrogen content of the high-hydrogen part of the couple was in the range of 500-2000 wppm, which was sufficient to maintain a two-phase mixture of hydride and saturated alpha solid solution during diffusion anneal. In this method, supersaturation of the low-hydrogen part of the couple was avoided since diffusion raised the level only to that of the alpha phase in the two-phase mixture. Hydrogen concentration in the equilibrated specimens was analyzed by the hot vacuum extraction method. The best-fit straight line through the data points for hydrogen solubility in annealed Zircaloy-2 and Zircaloy-4 was represented by an equation

$$\text{Solubility (wppm)} = 9.9 \times 10^4 \exp(-8250/RT) \qquad (2.1)$$

where R is the universal gas constant (1.987 cal/mol·K), and T is absolute temperature (Kearns, 1967). A representation of the hydrogen solubility as a function of reciprocal temperature is shown in Fig. 2.2. Hydrogen solubility values are 1, 71, 207, 460, and 851 wppm at 100, 300, 400, 500, and 600°C, respectively. It is believed that the solubility of hydrogen in Zircaloy-4 and Zirlo is similar in the temperature range of the present study.

The hydrogen concentration range in the current air-oxidation study of Zirlo is 100-1000 wppm, which indicates that some hydrogen will be present as hydride precipitates depending on temperature. By assuming that Zr hydride is a stoichiometric compound (ZrH_2) and the solubility of hydrogen is identical in Zircaloy-4 and Zirlo, we have calculated the total hydrogen content in the alloy as a function of volume fraction of hydride precipitates at 100-600°C. Figure 2.3 shows the total hydrogen content in the alloy as a function of hydride volume fraction. The calculations indicate that for a total hydrogen content of 1000 wppm, the volume fraction of hydride (at equilibrium) will be 0.055, 0.044, 0.03, and 0.005 at 100, 300, 500, and 600°C.

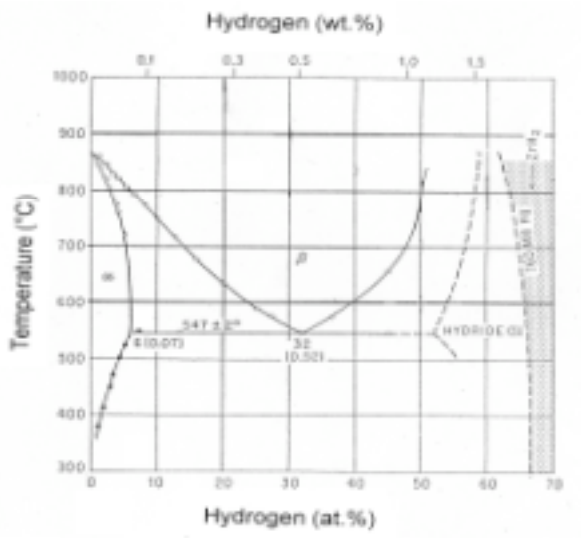

Figure 2.1. Zr-H phase diagram, indicating extremely low value for hydrogen solubility in Zr alloy (α phase) at the reactor operating temperature of 320°C.

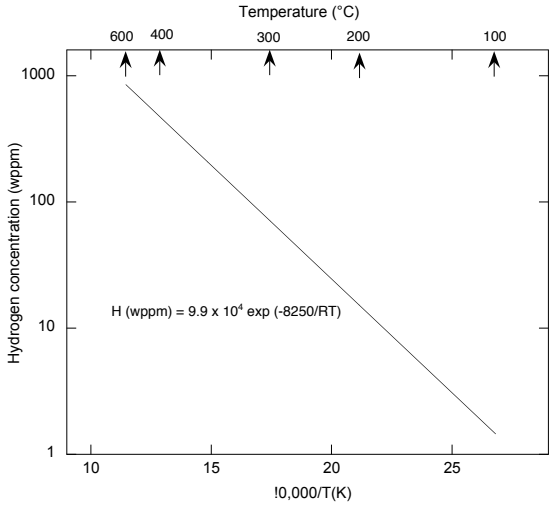

Figure 2.2. Solubility of hydrogen in Zircaloy-4 as a function of reciprocal temperature.

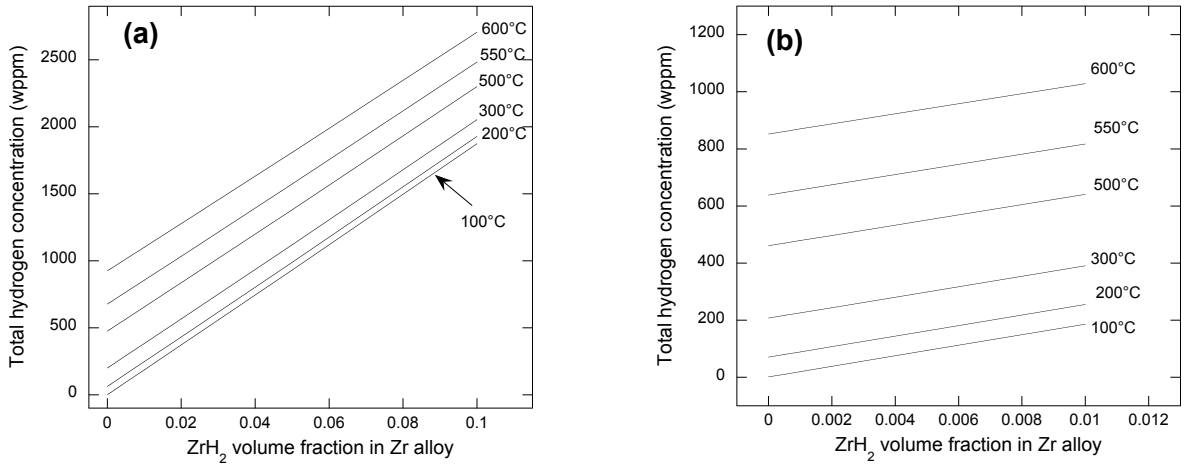

Figure 2.3. Total hydrogen concentration as a function of volume fraction of ZrH_2 phase at temperatures in the range of 100-600°C: (a) 0-0.1 ZrH_2 and (b) 0-0.01 ZrH_2.

3 Experimental Procedure

This section discusses the size and composition of the test material, type and geometry of the specimens used in various tests, and the facilities and approach for prehydriding, steam preoxidation, and air oxidation of the specimens.

3.1 Material

The Zirlo material used in the study was supplied by Westinghouse. The material, supplied in the form of tubes, had dimensions of 0.374 ± 0.0020 in. OD (9.45 ± 0.05 mm), and 0.328 ± 0.0015 in. ID (8.33 ± 0.038 mm), with an average wall thickness of 0.023 in. (0.58 mm). The chemical composition was determined by both Westinghouse and ANL, and the values are listed in Table 3.1.

Table 3.1. Chemical composition of Zirlo used in the study

Element[1]	Westinghouse analysis	ANL analysis[2]
Sn (wt.%)	0.99	0.73, 0.74
Fe (wt.%)	0.11	0.11, 0.12
Nb (wt.%)	0.98	0.96, 0.88
Cr (wt.%)	NR[3]	<0.01, <0.01
Si (wt.%)	0.005	<0.005, <0.005
Zr (wt.%)	Balance	Balance
Hf (wt ppm)	40	200, 200
C (wt ppm)	135	180, 90
O (wt ppm)	1100	1200, 1300
H (wt ppm)	NR	3.5, 5.7
N (wt ppm)	46	34, 36
Ni (wt ppm)	NR	<100, <100
Ta (wt ppm)	NR	<50, <50
W (wt ppm)	NR	<100, <100

[1]Units of measure in parentheses. [2]Duplicate analysis. [3]NR = Not reported.

3.2 Specimen Geometry

We used two types of specimens: rings ≈6.5 mm long and capsules 75 mm long. The ring specimens established the time for the prehydriding at 320°C to obtain the desired hydrogen concentration in the cladding, and the time and temperature for steam preoxidation of capsule specimens to obtain an oxide thickness ≈25-30 μm. Zirlo capsule specimens 75 mm in length were fabricated, and the capsules were back filled with argon gas and welded shut in a glove box. The capsule specimens were welded by e-beam on one side and tungsten inert gas (TIG) welding on the other side. The end caps were fabricated from Zircadyne 702 material. These specimens were used for air oxidation study in the initially prehydrided and prehydrided/steam-preoxidized conditions.

3.3 Prehydriding of Ring and Capsule Specimens

Hydrogen charging of ring and capsule samples of Zirlo was performed in two similar radiant-furnace systems, each equipped with a retort tube. Figure 3.1 shows a schematic of the

hydrogen-charging apparatus. Both systems are designed for experiments in hydrogen gas with flow rates up to 300 cc/min at pressures from atmospheric (0.10 MPa) to 0.12 MPa. Flow rates are computer controlled with Brooks mass-flow controllers. Furnace system-1 has a quartz retort tube that is 24-in (60-cm) long with a 2 in. (5-cm) I.D. It also has a uniform heat zone 6-in. (15-cm) long. System-2 has a 99.8% alumina retort tube that is 36-in (90-cm) long with a 3.5 in. (8.75-cm) I.D. It has a uniform heat zone that is 8 in. (20 cm) long. Both systems are able to maintain the temperature within 1°C of the desired value over the heat zone. System-1 is capable of 320°C heat-up in 15 min and cool-down to room temperature in 2 h. System-2 has a slower heat-up and cool-down due to its larger size. This condition also minimizes the thermal shock fracture of the alumina reaction tube.

System-1 was used primarily to conduct kinetic studies of the hydrogen charging process on ring specimens. System-2 was used for batch processing of Zirlo capsules for both hydrogen charging and steam preoxidation.

Zirlo ring and capsule samples were prepared for hydrogen charging by a light polishing with 1200-grit SiC paper to remove any surface oxides. They were then ultrasonically degreased with acetone followed by drying with a warm air blower. Figure 3.2 shows typical ring specimens after hydriding treatment at 320°C. Samples were weighed before and after hydrogen charging with a Mettler Model M5 microgram balance that has five-decimal-place precision. The difference yielded the hydrogen weight gain. Following weighing, the samples were placed on a holder assembly and inserted into the uniform heat zone of the retort tube such that the recording thermocouple well was at the midpoint of the holder assembly. The holder assemblies in furnace systems 1 and 2 were constructed of quartz and Alloy 625, respectively.

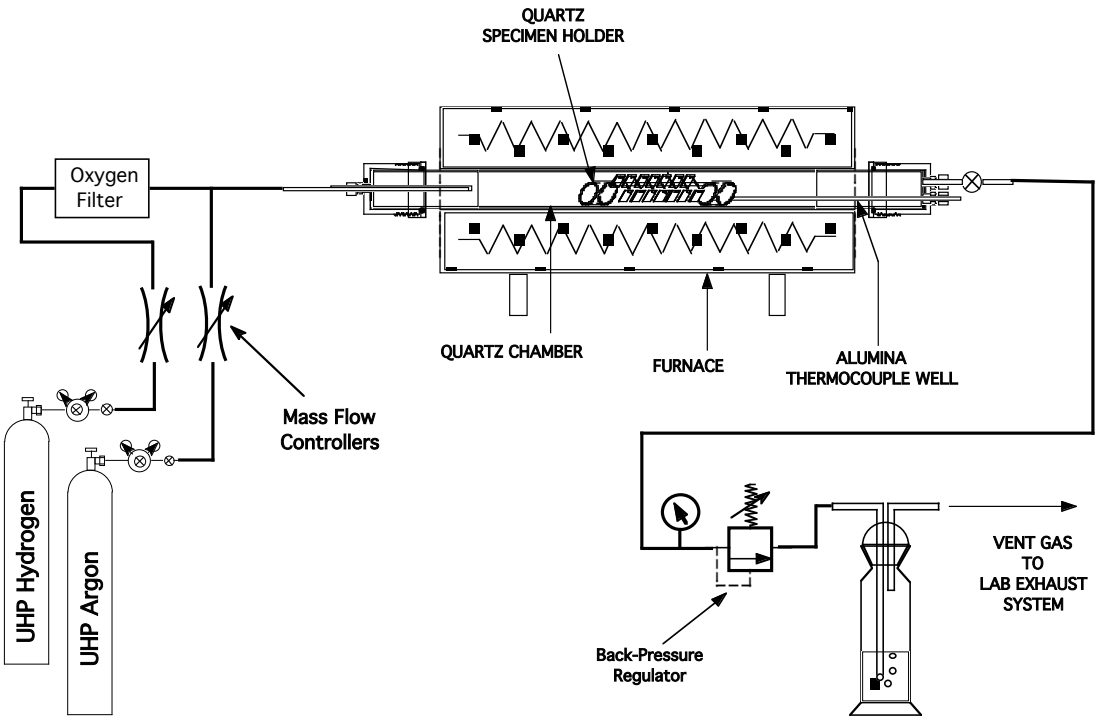

Figure 3.1. Test facility used for hydrogen charging of ring and capsule specimens of Zirlo.

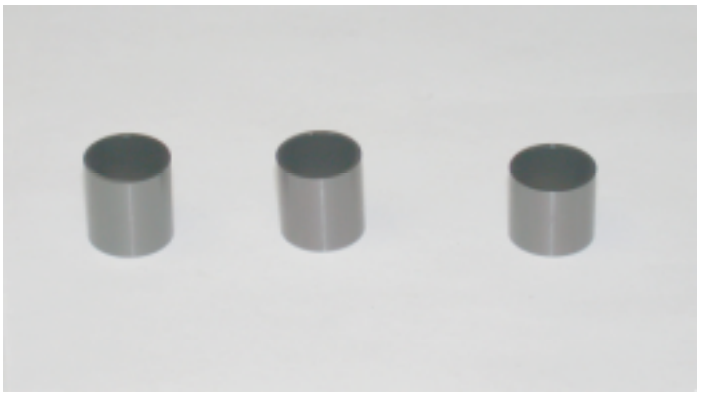

Figure 3.2. Typical ring specimens of Zirlo after exposure for hydriding at 320°C.

After loading the samples into the furnace retort chamber, the port opening was sealed closed with a Viton o-ring compression seal. The retort chamber was initially purged with ultra-high-purity (UHP) argon Gas (99.999 vol.%) at 200 cc/min flow rate for a minimum of 4 h at slightly above atmospheric pressure. Subsequently, the system was purged further by switching to research-grade hydrogen (99.9995 vol.%) at the 100 cc/min flow rate for 20 h. The hydrogen gas flowed through an oxygen absorbing gas-purifying filter (LabClear Model DGP-R1) prior to entering the retort chamber. After the purging period, the furnace was heated to 320°C in 15 min for the quartz chamber and 3 h for the alumina chamber to begin the hydrogen charging time.

Upon completion of the specimen exposure, the furnace was cooled down while hydrogen gas flow was maintained at the test flow rate. The system-1 quartz chamber was cooled to room temperature in ≈2 h, while the alumina chamber in system-2 required ≈4 h cool down period. At room temperature, hydrogen gas was flushed out of the retort chambers with UHP argon gas at a flow rate of 200 cc/min for 30 min. Furnace chambers were then vented, and hydrogen-charged specimens were retrieved for visual inspection and weight-gain determination. Samples were stored in polyethelene bags for future steam preoxidation and/or air oxidation. Figure 3.3 shows capsule specimens of Zirlo before (left figure) and after hydriding exposure for 170 h in hydrogen gas at 320°C (right figure).

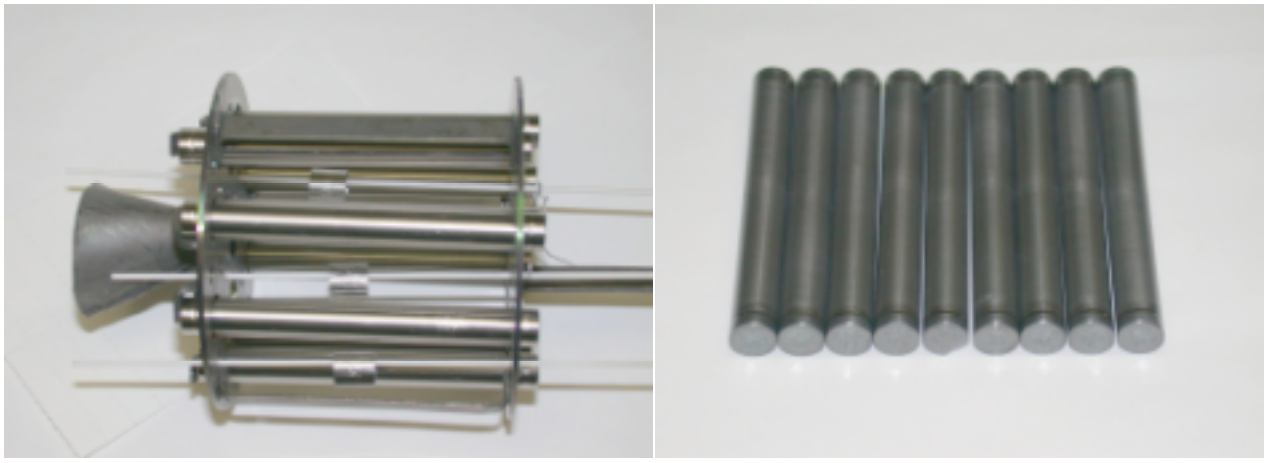

Figure 3.3. Capsule specimens of Zirlo (75-mm long) before (in holder) and after hydriding treatment. Dark gray color: as fabricated; dark black color: after 170-h exposure in hydrogen gas at 320°C.

3.4 Steam Exposure of Prehydrided Ring and Capsule Specimens

Two tubular resistance-heated furnaces were used to expose the ring and capsule specimens to steam oxidation. Figure 3.4 shows one of the facilities used for steam oxidation. The system consists of a resistance-heated furnace with a constant temperature zone of ≈20 cm. The reaction chamber was made of high-purity alumina. The steam for the experiment was generated by pumping distilled water from a water source and converting it to steam in the preheat portion of the furnace, ahead of the specimen exposure location. The exhaust steam from the chamber was condensed in a steam condenser. The flow rate was 6 cc/h of water. A mass balance on the water flow showed that almost all the input water was collected as the effluent, indicating that the steam consumption was negligible during the oxidation of specimens. Argon gas was used to disperse the steam in the reaction chamber.

3.5 Air Exposure

Four resistance-heated furnaces were used for oxidation of prehydrided and prehydrided/steam-preoxidized zirlo capsule specimens in air. The capsules were retrieved periodically to measure the weight changes and determine the oxide thickness by optical metallography.

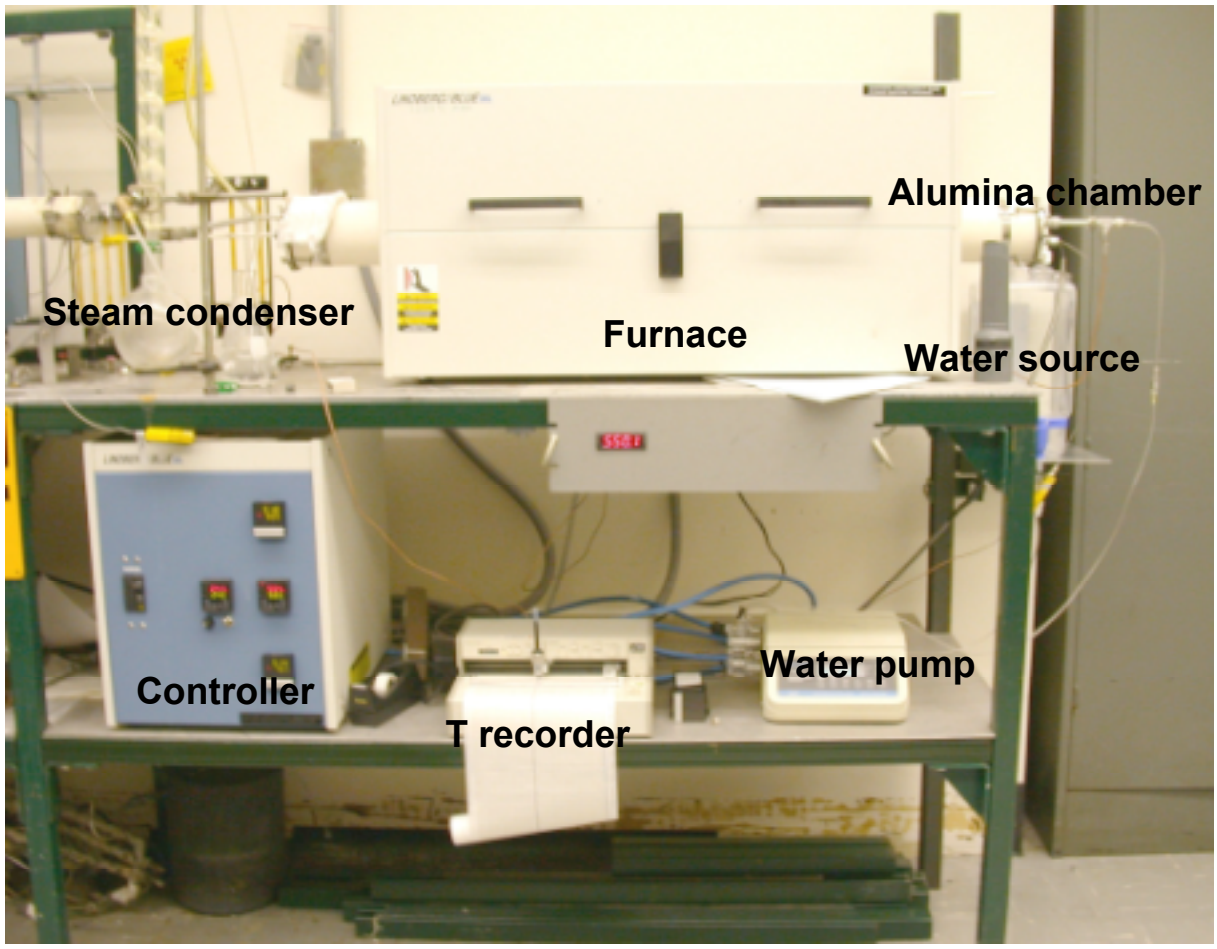

Figure 3.4. Test facility used for steam preoxidation of prehydrided Zirlo specimens.

For the prehydrided/steam-preoxidized specimens that were subsequently exposed in air, the specimens after each exposure time were cut, mounted, polished, and analyzed by scanning electron microscopy (SEM) to determine the total oxide thickness and that developed during the air exposure step. Total oxide thickness was measured in the four quadrants around the capsule specimen, and the values were averaged to establish the scale thickness. Oxide growth during air exposure was calculated from the measured weight change.

4 Prehydriding of Zirlo

4.1 Gas Phase Hydriding

Ring specimens of Zirlo were hydrided in 99.9995 vol.% hydrogen gas at 320°C, the details of which were presented in Section 3.3. Table 4.1 lists the H concentration values obtained on various ring specimens after exposure to hydrogen gas at 320°C. Figure 4.1 shows the hydrogen concentrations obtained on several ring specimens as a function of exposure time. Based on this information, conditions of 170 h at 320°C were selected for the exposure of Zirlo capsule specimens to obtain a hydrogen concentration of 600 wppm, typical of levels anticipated under high-burnup condition.

Table 4.1. Hydrogen concentration in Zirlo rings after prehydriding treatment in hydrogen gas

Specimen Number	Exposure time in hydrogen gas (h)	Measured hydrogen concentration (wppm)	Specimen Pretreatment	Hydrogen Analysis Performer
ZRL-1	-	3.5	As-received	CONAM
ZRL-2	-	5.7	As-received	CONAM
ZLH-A	6.3	90.6	None	Staveley
ZLH-B	12.4	92.7	None	Staveley
ZLH-C	28.4	175.0	None	Staveley
ZLH-D	68.4	321.0	None	Staveley
ZLH-D	68.4	360.0	None	Staveley
ZLH-E	64.2	202.0	None	Staveley
ZLH-F	24.2	187.0, 202.0[1]	None	ANL

[1]Duplicate analysis.

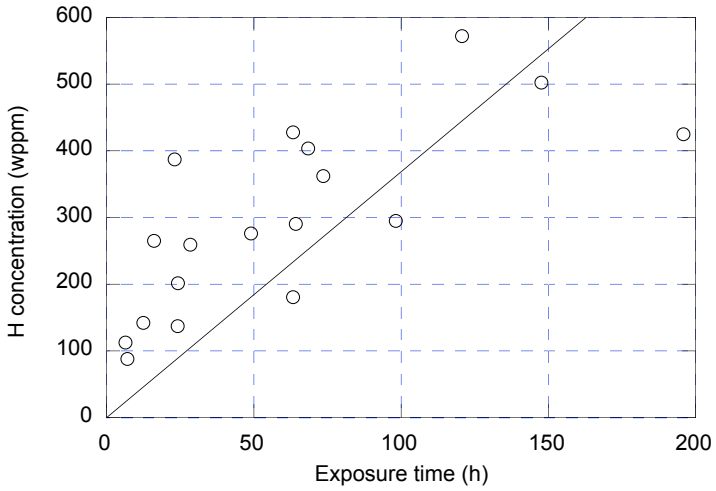

Figure 4.1. Hydrogen concentration in Zirlo ring specimens as a function of exposure time in pure hydrogen gas at 320°C.

4.2 Hydriding in Steam

We also exposed several ring specimens of Zirlo in a steam environment at 550°C for several time periods. Our goal was to examine the hydrogen ingress into the material from steam exposure and also to establish the oxide thickness for the exposed specimens. These specimens were also analyzed for hydrogen content, and the oxide thickness was calculated from the weight change. Figure 4.2 shows the hydrogen concentration and oxide thickness for the Zirlo ring specimens as a function of exposure time in steam at 550°C. Based on these data, prehydriding of bare capsules was followed by steam exposure to obtain 30-μm-thick oxide. The hydrogen content of these specimens is expected to be higher than 600 wppm, and the results from these exposures are discussed in a later section.

Table 4.2. Oxide thickness and hydrogen concentration in Zirlo rings after steam exposure

Specimen Number	Exposure time (h)	Weight change (mg/mm^2)	Measured ZrO_2 oxide thickness (μm)	Measured hydrogen concentration (wppm)	Average hydrogen concentration (wppm)
AR	0	-	-	5.0	5.0
ZRL-H	144.0	3.7×10^{-2}	24.6	1265, 1156[1]	1211
ZRL-J	139.5	3.9×10^{-2}	27.0	1311, 1204[1]	1258
ZRL-K	48.0	1.1×10^{-2}	10.8	223, 197[1]	210
ZRL-L	15.9	5.5×10^{-3}	4.7	20.3	20.3
ZRL-M	33.1	9.5×10^{-3}	8.3	122	122
ZRL-N	62.6	1.8×10^{-2}	12.8	569	569
ZRL-O	129.4	3.7×10^{-2}	25.9	1252	1252
ZRL-P	178.4	5.2×10^{-2}	38.6	1574	1574
ZRL-R	254.9	7.2×10^{-2}	46.7	2221	2221

[1]Duplicate analysis; these were performed by LECO Corporation, and all others were performed at ANL.

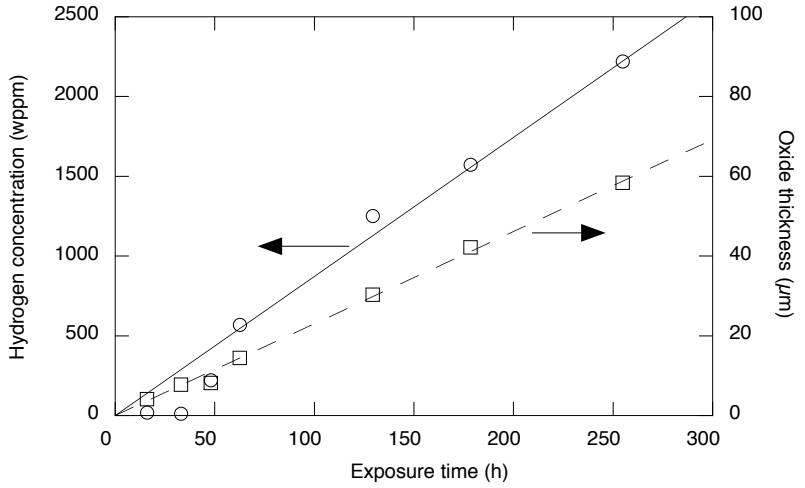

Figure 4.2. Hydrogen concentration and ZrO_2 thickness in Zirlo ring specimens as a function of exposure time in steam at 550°C.

An attempt was made to correlate the oxide scale thickness with the hydrogen concentration in the alloy and examine the role of dissolved oxygen in the water/steam. In our steaming experiments, water (in the aerated condition) was pumped into the furnace and converted into steam prior to reaction with the Zirlo specimens. As a result, there are two possible reactions (extreme cases) that can lead to hydrogen ingress into the alloy:

$$Zr + 2H_2O = ZrO_2 + 4H \text{ (deaerated condition)} \quad (4.1)$$

$$Zr + H_2O + 1/2\ O_2 = ZrO_2 + 2H \text{ (aerated condition)} \quad (4.2)$$

Figure 4.3 shows a plot of measured and calculated hydrogen concentrations as a function of oxide thickness for Zilro specimens after steam exposure. Also shown in the figure are the lines that correspond to expected hydrogen in the alloy for oxide thicknesses based on reactions (4.1) and (4.2).

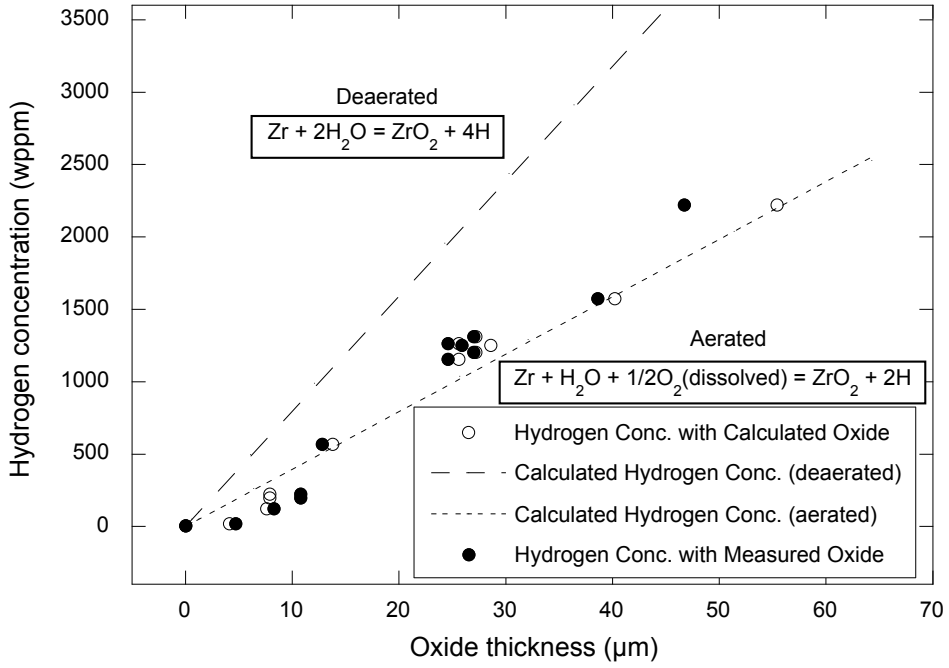

Figure 4.3. Hydrogen concentration as a function of oxide thickness for Zilo specimens steam oxidized at 550°C.

4.3 Hydriding of Capsules

Based on the H ingress data on ring specimens, we hydrided several 75-mm-long capsules of Zirlo in a pure hydrogen gas at 320°C for 170 h. Figure 4.4 shows the weight gain for 14 capsules from two exposure runs that were conducted to prehydride the Zirlo capsules. The weight change for the capsules ranged between 6×10^{-4} and 1.1×10^{-3} mg/mm^2. The prehydrided capsules were used in subsequent tests for air oxidation with and without steam preoxidation.

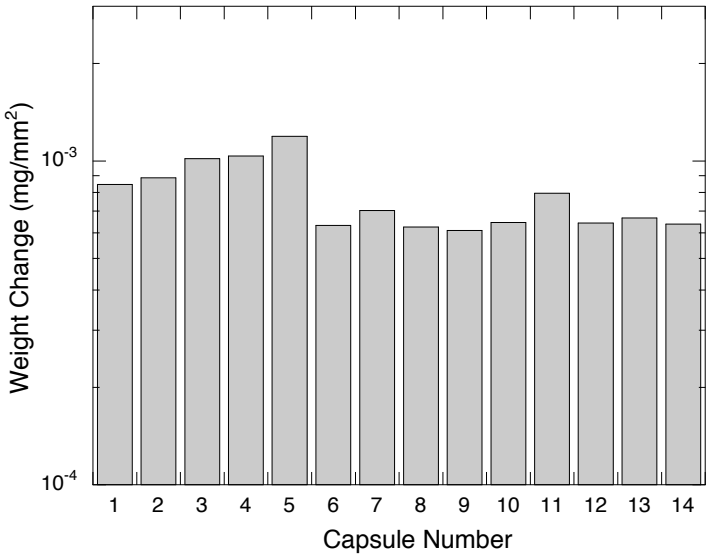

Figure 4.4. Weight change in 75-mm-long capsule specimens after 170-h exposure in pure hydrogen gas at 320°C.

5 Air Oxidation of Prehydrided Zirlo

Prehydrided capsules 1-4 were selected for the air oxidation study at 300, 400, 500, and 600°C. The specimens were retrieved periodically to measure the weight change of the capsules. The exposure times for these capsules ranged from a maximum of 1000 h at 300°C to 300 h at 600°C. Tables 5.1 and 5.2 list the air oxidation data generated at various temperatures and the measured concentrations for hydrogen, oxygen, and nitrogen in all the specimens tested. Upon completion of the air exposures, the specimens were analyzed for their hydrogen content by bulk analysis and for hydrogen distribution by metallography.

Figure 5.1 shows the weight change data obtained at 300-600°C during air oxidation of Zirlo capsules, that were prehydrided for 170 h in hydrogen gas at 320°C. Also shown in the figure are the air oxidation data developed earlier for bare Zirlo that contained ≈5 wppm hydrogen (Natesan and Soppet, 2004). The results indicate that at hydrogen concentrations in the range of 116 to 329 wppm (measured in these prehydrided capsules – see Table 5.1), hydrogen has virtually no effect on air oxidation kinetics. Figure 5.2 shows the weight change data obtained at 300-600°C during air oxidation of bare Zirlo capsules and Zirlo rings that were prehydrided for 452 h in H_2 gas at 320°C. Note that the sealed capsules of the bare alloy were air oxidized on the OD side only, whereas the prehydrided ring specimens were oxidized on both the OD and ID of the specimens. The data in Figs. 5.1 and 5.2 are normalized with respect to area, and therefore, the weight change can be directly compared. Again, the rates are comparable for both bare and prehydrided specimens at all temperatures except 600°C, where the weight gain is slightly higher for prehydrided specimens.

Table 5.1. Air oxidation data for Zirlo capsules that were prehydrided in hydrogen gas for 170 h at 320°C

Specimen Number	Exposure temperature in air (°C)	Exposure time in air (h)	Weight change (mg/mm^2)	Calculated ZrO_2 thickness (μm)	Measured hydrogen concentration (wppm)	Measured oxygen concentration (wt.%)	Measured nitrogen concentration (wppm)
ZLC-38	-	-	-	-	170, 172	-	-
ZLC-34	300	120	9.2×10^{-4}	0.1	-	-	-
		310	2.1×10^{-4}	0.1	-	-	-
		621	3.5×10^{-4}	0.2	-	-	-
		1026	4.4×10^{-4}	0.3	138, 130	0.144, 0.142	29, 26
ZLC-35	400	75	7.5×10^{-4}	0.5	-	-	-
		166	1.2×10^{-3}	0.8	-	-	-
		332	1.8×10^{-3}	1.2	-	-	-
		666	3.1×10^{-3}	2.1	118, 116	0.194, 0.191	32, 32
ZLC-36	500	50	5.6×10^{-3}	3.8	-	-	-
		100	7.8×10^{-3}	5.3	-	-	-
		260	1.7×10^{-2}	11.3	-	-	-
		425	3.0×10^{-2}	20.8	-	-	-
		500	3.6×10^{-2}	24.7	157, 156	0.848, 0.952	53, 54
ZLC-37	600	40	3.4×10^{-2}	22.7	-	-	-
		80	7.3×10^{-2}	48.8	-	-	-
		150	1.5×10^{-1}	96.6	-	-	-
		316	3.6×10^{-1}	221.7	249, 329	4.45, 7.43	298, 300

Table 5.2. Air oxidation results for 25-mm-long ring samples of Zirlo that were prehydrided in hydrogen gas for 452 h at 320°C

Specimen Number	Exposure temperature in air (°C)	Exposure time in air (h)	Weight change (mg/mm^2)	Calculated ZrO_2 thickness (μm)	Measured hydrogen concentration (wppm)
LHAE	300	100	1.1×10^{-4}	0.1	-
		295	1.8×10^{-4}	0.1	-
		607	1.2×10^{-3}	0.8	-
		1010	2.2×10^{-3}	1.5	88
LHAD	400	75	5.5×10^{-4}	0.4	-
		146	1.0×10^{-3}	0.7	-
		297	1.4×10^{-3}	1.0	-
		609	2.3×10^{-3}	1.6	53.4, 53.5
LHAK	500	50	5.0×10^{-3}	3.3	-
		101	6.3×10^{-3}	4.3	-
		248	1.4×10^{-2}	9.7	-
		536	3.1×10^{-2}	21.4	101.8, 100
LHAM	600	43	4.3×10^{-2}	29.5	-
		59	6.1×10^{-2}	41.9	-
		80	8.4×10^{-2}	57.9	
		150	1.7×10^{-1}	114.6	-
		302	3.7×10^{-1}	254.9	350.6, 360.2

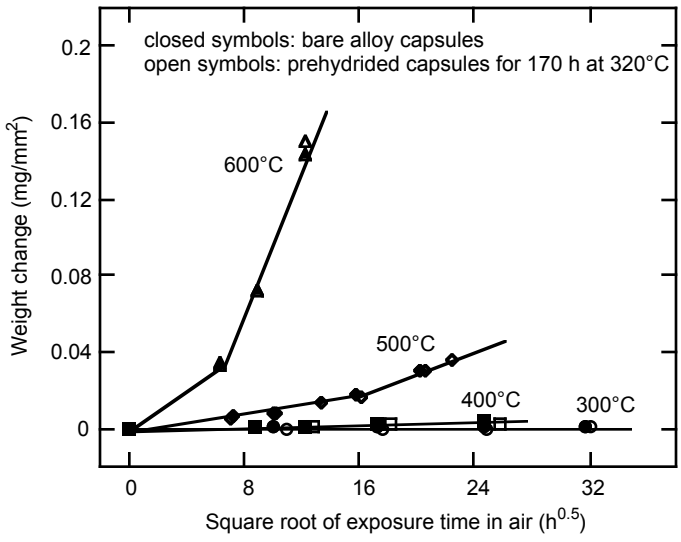

Figure 5.1. Weight change during air oxidation in capsule specimens of bare and prehydrided Zirlo after 170-h exposure in pure hydrogen gas at 320°C.

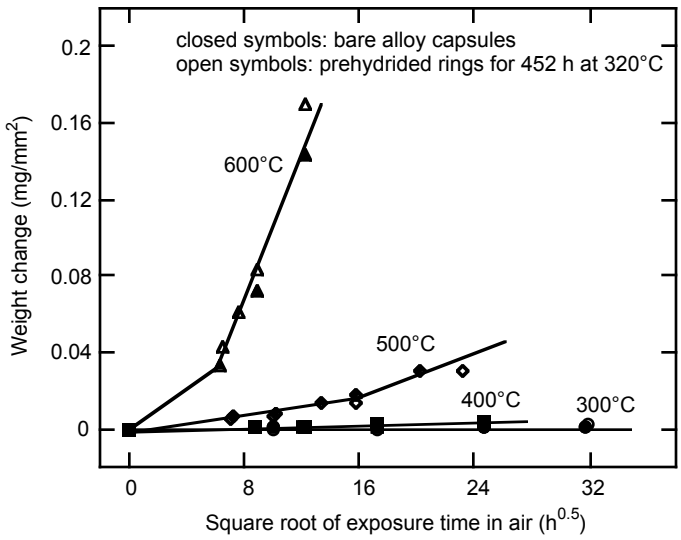

Figure 5.2. Weight change during air oxidation in capsule specimens of bare Zirlo specimens and in ring specimens of prehydrided Zirlo that were exposed for 452 h in pure hydrogen gas at 320°C.

Figures 5.3-5.5 show cross sections of Zirlo capsules that were prehydrided at 320°C, prehydrided at 320°C/air oxidized for 500 h at 500°C, and prehydrided at 320°C/air oxidized for 316 h at 600°C. The prehydrided specimen containing ≈170 wppm hydrogen (which exceeds the solubility value of 90 wppm at 320°C) exhibited small circumferential stringers of ZrH_2 precipitate. However, these hydrides dissolved in the matrix (note absence of precipitates in Figures 5.4 and 5.5) during air exposure at 500 and 600°C since the hydrogen solubility is much higher than 90 wppm at these higher temperatures. The oxide thicknesses observed upon air oxidation of the prehydrided specimens were similar to those observed during air oxidation of bare Zirlo specimens, the results of which were reported extensively in an earlier report (Natesan and Soppet, 2004). For example, the measured oxide thickness for the prehydrided alloy was 25.6 μm (calculated value was 24.7 μm) after 500-h oxidation at 500°C, whereas the corresponding value for bare alloy was 21.7 μm after 412-h oxidation at 500°C. Similarly, the measured oxide thickness for the prehydrided alloy was 228.1 μm (calculated value was 221.7 μm) after 316-h oxidation at 600°C, whereas the corresponding value for bare alloy was 219.4 μm after 313-h oxidation at 600°C.

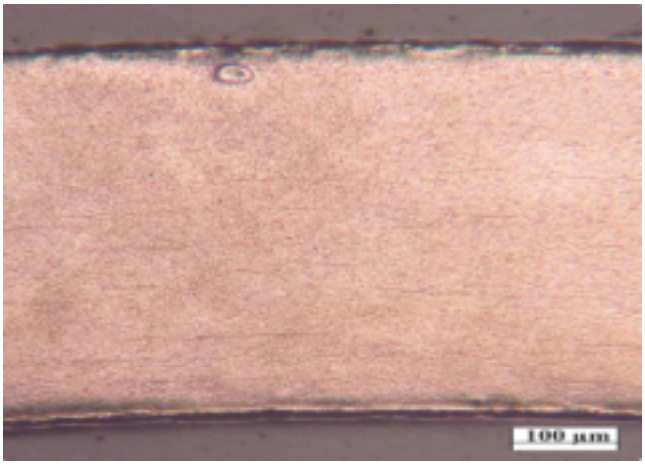

Figure 5.3. SEM photomicrograph of cross section of Zirlo capsule prehydrided for 170 h at 320°C.

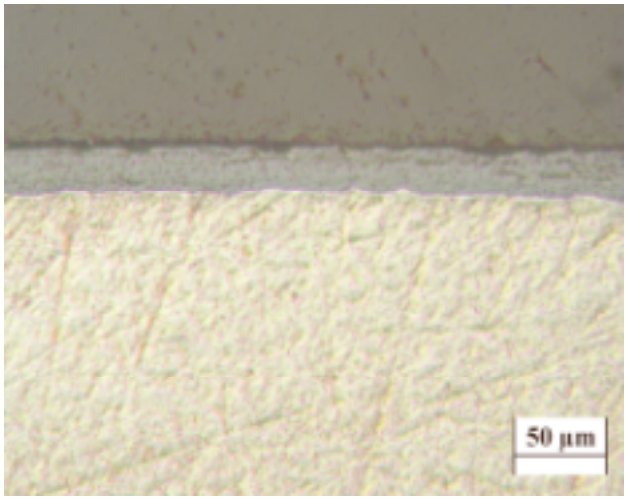

Figure 5.4. SEM photomicrograph of cross section of initially prehydrided Zirlo capsule, after air oxidation for 500 h at 500°C.

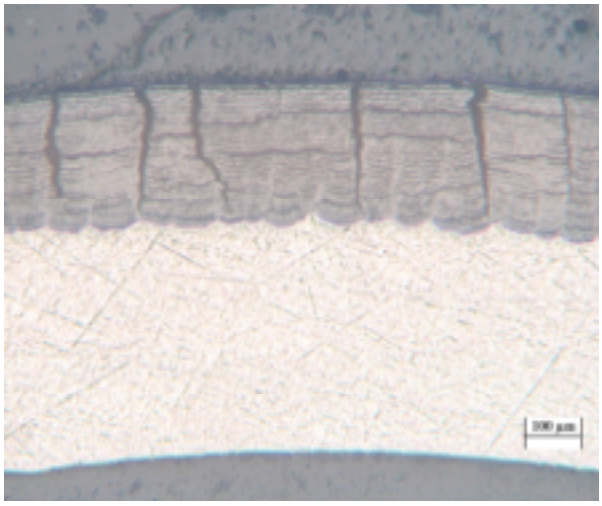

Figure 5.5. SEM photomicrograph of cross section of initially prehydrided Zirlo capsule, after air oxidation for 316 h at 600°C.

6 Air Oxidation of Prehydrided and Steam-Preoxidized Zirlo

Several prehydrided capsule specimens were steam oxidized at 550°C for 140 h (a condition that was used in earlier study) to develop ≈25-μm-thick oxide on the prehydrided specimens. Two capsules were exposed in air at each of the four temperatures of 300, 400, 500, and 600°C. These specimens were retrieved periodically to measure their weight changes. The exposure times for these capsules ranged from a maximum of 1000 h at 300°C to 300 h at 600°C. At each temperature, one capsule was retrieved at an intermediate exposure time and destructively analyzed to establish the oxide thickness. Table 6.1 lists the air oxidation data generated at various temperatures and the measured concentrations for hydrogen, oxygen, and nitrogen in all the prehydrided/steam-preoxidized specimens tested. It is evident that prehydriding/steam preoxidation results in hydrogen concentration of ≈733 wppm (see specimen number ZLC-47 in Table 6.1). Air oxidation of these capsules at 300-500°C did not significantly increase the hydrogen concentration. At 600°C and exposure times >150 h, where significant cracking of the oxide scales is anticipated, the capsules showed somewhat larger hydrogen concentration than the starting value of ≈733 wppm.

Figure 6.1 shows weight change data obtained at 500 and 600°C during air oxidation of specimens that were initially either only steam oxidized or prehydrided/steam-oxidized to obtain ≈25-μm-thick oxide. The prehydriding condition was 170 h at 320°C. The steam oxidation condition was 140 h at 550°C. The data indicate virtually no effect of prehydriding on air oxidation at 500°C and slightly beneficial effect at 600°C. Figure 6.2 shows weight change data

Table 6.1. Air Oxidation results for Zirlo capsules that were prehydrided in hydrogen gas for 170 h at 320°C and steam preoxidized for 140 h at 550°C

Specimen Number	Exposure temperature in air (°C)	Exposure time in air (h)	Weight change in air (mg/mm^2)	Calculated ZrO_2 thickness (μm)	Measured ZrO_2 thickness in steam and in air (μm)	Measured hydrogen concentration (wppm)	Measured oxygen concentration (wt.%)	Measured nitrogen concentration (wppm)
ZLC-47	-	-	-	-	23.7	729, 737[1]	1.00, 0.85[1]	46, 57[1]
ZLC-39	300	96	5.7×10^{-4}	0.4		-	-	-
		305	1.5×10^{-3}	1.0		-	-	-
		615	2.0×10^{-3}	1.4		-	-	-
		973	2.3×10^{-3}	1.6	25.8	774, 779	1.07, 1.11	46, 45
ZLC-41	400	73	1.9×10^{-3}	1.3		-	-	-
		160	2.8×10^{-3}	1.9		-	-	-
		326	3.8×10^{-3}	2.6	27.9	739, 748	1.14, 1.15	43, 43
		636	5.4×10^{-3}	3.7	28.9	752, 757	1.09, 1.09	47, 47
ZLC-43	500	50	3.8×10^{-3}	2.6		-	-	-
		100	7.6×10^{-3}	5.2		-	-	-
		262	5.6×10^{-2}	14.1	37.2	752, 764	1.38, 1.45	75, 61
		500	4.0×10^{-2}	27.5	49.6	775, 784	1.91, 1.96	71, 67
ZLC-46	600	40	4.2×10^{-2}	27.9	50.1	726, 747	2.08, 1.61	84, 67
		80	8.7×10^{-2}	56.4		-	-	-
		150	1.7×10^{-1}	104.6	137.4	765, 881	5.05, 4.90	164, 163
		315	3.9×10^{-1}	216.3	269.2	849, 1136	8.85, 9.13	294, 298

[1]Duplicate analysis.

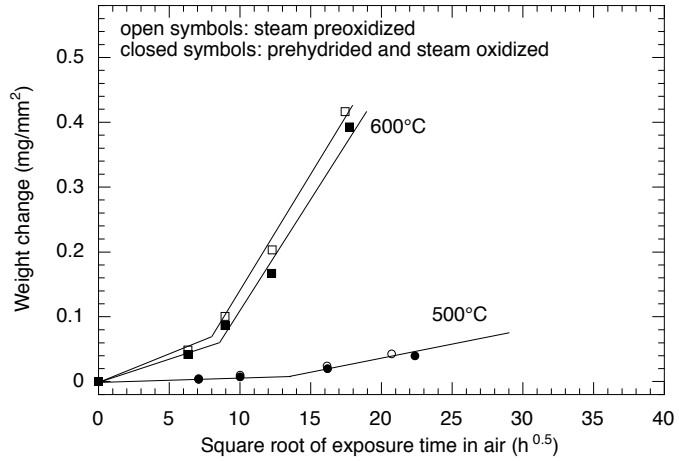

Figure 6.1. Weight change data obtained at 500 and 600°C during air oxidation of Zirlo capsule specimens that were initially either only steam oxidized or prehydrided/steam oxidized.

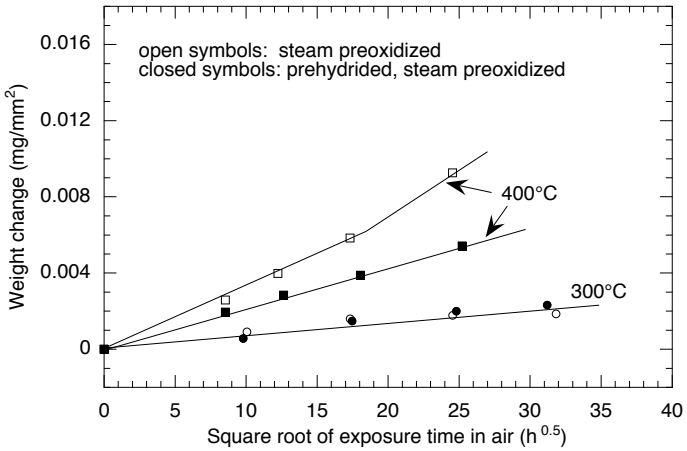

Figure 6.2. Weight change data obtained at 300 and 400°C during air oxidation of Zirlo capsule specimens that were initially either only steam oxidized or prehydrided/steam oxidized.

obtained in air oxidation at 300 and 400°C. Results show that, at 300°C for up to 1000 h, the effect of prehydriding has virtually no effect on subsequent air oxidation. At 400°C, the prehydriding seems to have a beneficial effect in reducing the oxidation rate during subsequent air exposure. Figures 6.3 and 6.4 show the calculated oxide thickness for air-oxidized specimens that were initially either only steam oxidized or prehydrided/steam oxidized.

Figures 6.5 and 6.6 show scanning electron microscopy (SEM) photomicrographs of cross sections of a Zirlo specimen in the as-received condition and a prehydrided specimen that was oxidized in air for 1026 h at 300°C. The latter specimen had an hydrogen concentration of ≈135 wppm, which exceeds the solubility value at 320°C. The microstructure clearly shows precipitates of hydrides in the circumferential orientation across the entire cladding thickness, indicating that once the hydrides are precipitated, subsequent oxidation occurs at low temperatures such as 300°C has little effect on its distribution. Also shown in these figures are Knoop hardness indentations that were made at several locations across the cladding thickness. The size of the indentations within each specimen shows very little variation, indicating negligible variation in hardness. Figures 6.7 and 6.8 show SEM photomicrographs of cross sections of Zirlo specimens in steam-preoxidized/air-oxidized and prehydrided/steam-preoxidized/air-oxidized conditions, respectively. Both these specimens were oxidized in air for ≈1000 h at 300°C. The measured hydrogen concentrations in these specimens were 695 and

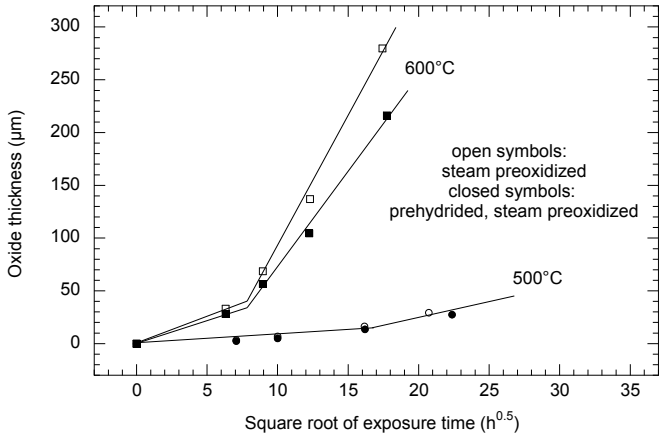

Figure 6.3. Oxide thickness data obtained at 500 and 600°C during air oxidation of Zirlo capsule specimens that were initially either only steam oxidized or prehydrided/steam oxidized.

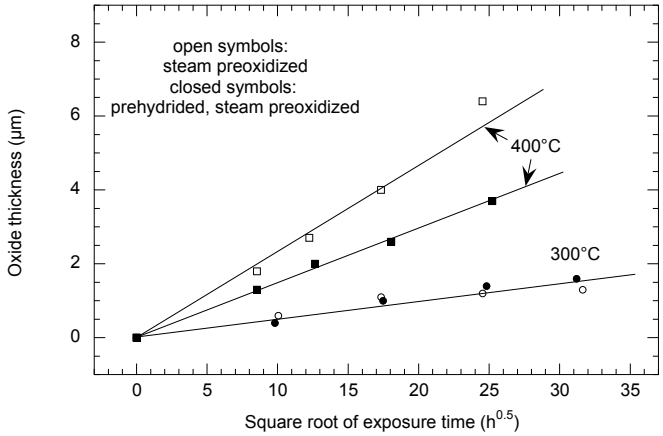

Figure 6.4. Oxide thickness data obtained at 300 and 400°C during air oxidation of Zirlo capsule specimens that were initially either only steam oxidized or prehydrided/steam oxidized.

776 wppm, respectively. Knoop hardness indentations that were made at several locations across the cladding thickness in these specimens also exhibited negligible variation.

Figure 6.9 shows Knoop hardness profiles as a function of cladding thickness for an as-received Zirlo specimen. Measurements were made in four quadrants of the tube, and they indicate significant variation in hardness between the quadrants but also in the radial direction within each quadrant. Figure 6.10 shows similar hardness profiles obtained for an initially steam-preoxidized Zirlo after 1000-h exposure in air at 300°C. Steam preoxidation at 550°C for 140 h seems to homogenize the material with a resultant uniformity in hardness values in all four quadrants and across the cladding wall. Figure 6.11 shows a composite plot of hardness profile data developed for Zirlo with several pretreatments and air oxidation. The hydrogen concentrations in these specimens ranged between 5 and 735 wppm. The data in Fig. 6.11 indicate that the exposure of the Zirlo specimen at elevated temperature (e.g., steam preoxidation at 550°C) has a much more softening effect than the hardening effect that can result from higher hydrogen content (e.g., 695 and 735 wppm in steam-oxidized specimens).

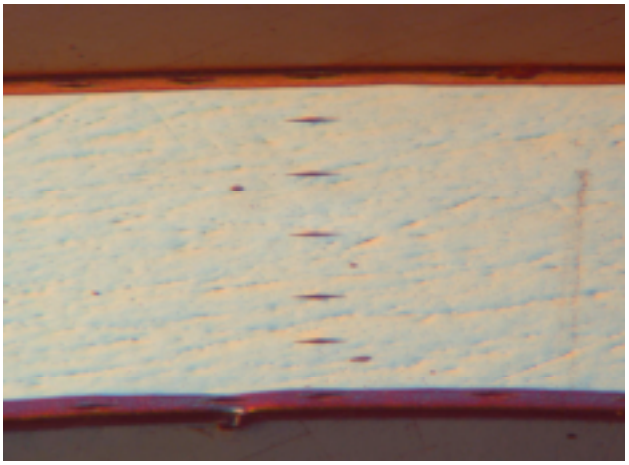

Figure 6.5. Knoop microhardness indentations on as-received Zirlo cladding tube.

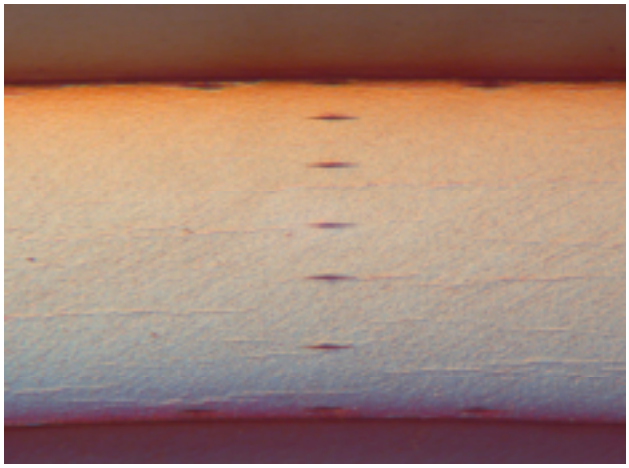

Figure 6.6. Knoop microhardness indentations on initially prehydrided Zirlo cladding tube after 1026-h air oxidation at 300°C.

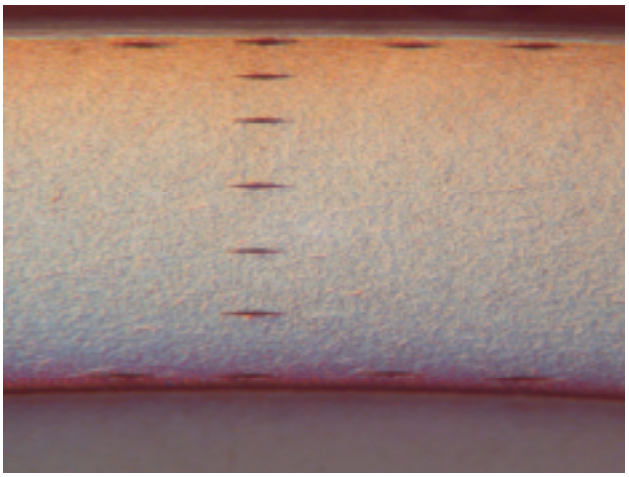

Figure 6.7. Knoop microhardness indentations on initially steam-oxidized (for 140 h at 550°C) Zirlo cladding tube after 1000-h air oxidation at 300°C.

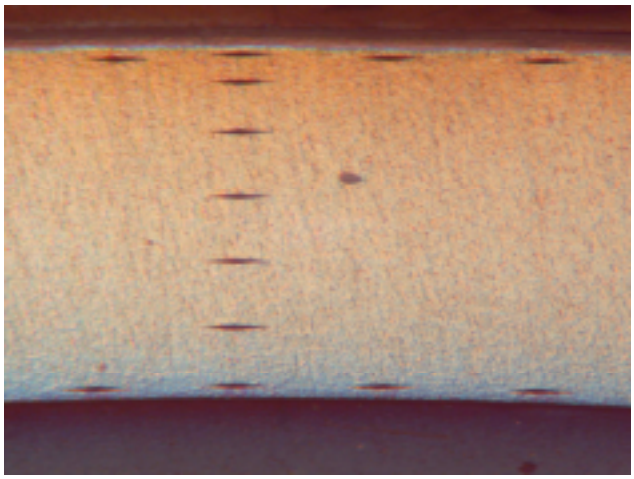

Figure 6.8. Knoop microhardness indentations on initially prehydrided/steam-oxidized Zirlo cladding tube after 973-h air oxidation at 300°C.

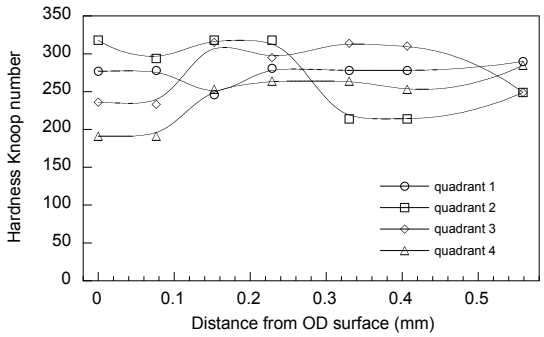

Figure 6.9. Knoop hardness profiles for as-received Zirlo in four quadrants.

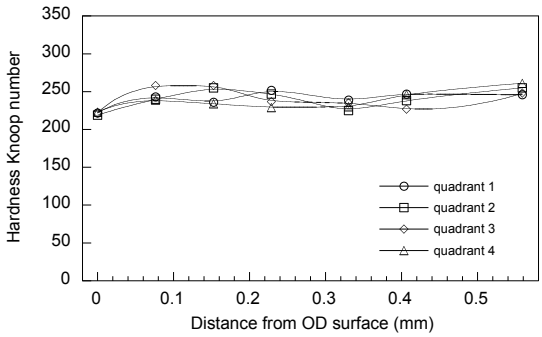

Figure 6.10. Knoop hardness profiles in four quadrants for initially steam-preoxidized Zirlo after 1000-h exposure in air at 300°C.

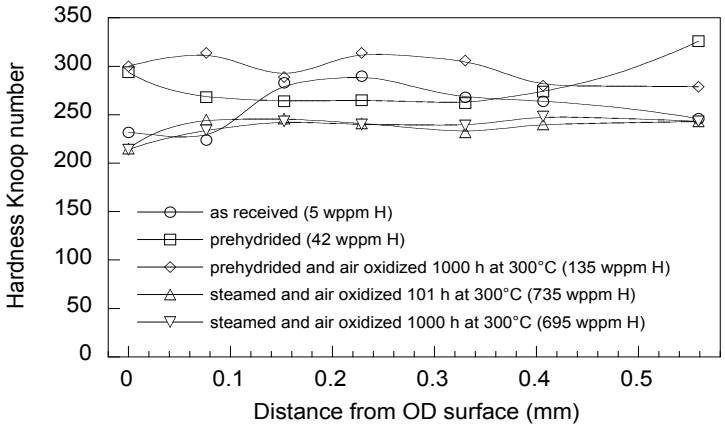

Figure 6.11. Knoop hardness profiles for Zirlo in as-received condition and after several treatments. Hydrogen concentrations in different specimens are given in the legend.

7 Correlations for Oxidation Kinetics

In general, the kinetics of oxidation of Zirlo specimens were derived from weight change data by plotting the weight change against square root of exposure time and fitting the data by two lines to depict pre- and post-breakaway kinetics. The slopes of both fitted lines were calculated and were used to determine rate constants for the oxidation process. The rates developed using the weight change data at different temperatures were curve fitted in an Arrhenius-type formalism,

$$\text{Rate constant} = A \exp(-B/TK) \quad (7.1)$$

where A and B are constants, and TK is temperature in degrees Kelvin.

Equations for the air oxidation of steam-preoxidized Zirlo specimens in the low-temperature range (Natesan and Soppet, 2004) are

$$\text{Rate constant } (kg^2/m^4 \cdot s) = 0.07 \exp(-14430/TK) \text{ for pre-breakaway, } 573 \le TK \le 873 \quad (7.2)$$

$$\text{Rate constant } (kg^2/m^4 \cdot s) = 8.3 \times 10^4 \exp(-24000/TK) \text{ for post-breakaway, } 673 \le TK \le 873 \quad (7.3)$$

Equations for the air oxidation of bare Zirlo specimens in the low-temperature range are

$$\text{Rate constant (in } kg^2/m^4 \cdot s) = 0.057 \exp(-14240/TK) \text{ for pre-breakaway, } 573 \le TK \le 873 \quad (7.4)$$

$$\text{Rate constant (in } kg^2/m^4 \cdot s) = 1.0 \times 10^5 \exp(-24580/TK) \text{ for post-breakaway, } 673 \le TK \le 873 \quad (7.5)$$

Correlations were also developed to depict the kinetics of oxide scale growth over the temperature range of 300-600°C. Equations for oxide growth are as follows:

$$\text{Oxide growth rate constant } (\mu m^2/s) = 2662 \exp(-12790/TK) \text{ for pre-breakaway, } 573 \le TK \le 873 \quad (7.6)$$

$$\text{Oxide growth rate constant } (\mu m^2/s) = 1.44 \times 10^8 \exp(-19610/TK) \text{ for post-breakaway, } 673 \le TK \le 873 \quad (7.7)$$

Since we acquired limited data on the air oxidation kinetics of prehydrided and prehydrided/steam-preoxidized Zirlo specimens, an attempt was made to compare the data from this program with extensive oxidation database developed earlier on bare and steam-preoxidized Zirlo specimens (Natesan and Soppet, 2004). The parabolic rate constants and oxide-growth rate constants from the current program are listed in Table 7.1, along with the data obtained earlier on bare and steam-preoxidized Zirlo. Further, the data from this program were used to evaluate, if any, the role of hydrogen content in the alloy in its behavior during air exposure.

Figure 7.1 shows a plot of parabolic rate constant for oxidation of Zirlo in the pre-breakaway region, as a function of hydrogen content in the alloy, irrespective of whether the hydrogen ingress was achieved by prehydriding in hydrogen gas or during steam preoxidation. A similar plot of parabolic rate constant for oxidation in the post-breakaway region is shown in Fig. 7.2. The data indicate that rates may be somewhat lower for hydrogen contents of

Table 7.1. Parabolic rate constants, based on weight change and oxide thickness, for air oxidation of Zirlo cladding with various pretreatments

Initial condition	Air oxidation temperature (°C)	Parabolic rate constant ($kg^2/m^4 \cdot s$)		Oxide thickness rate constant ($\mu m^2/s$)	
		Pre-breakaway	Post-breakaway	Pre-breakaway	Post-breakaway
Steam preoxidized[1]	900	1.8×10^{-6}	5.7×10^{-5}	2.8×10^{-2}	3.8
	800	3.1×10^{-7}	1.2×10^{-5}	1.9×10^{-2}	2.6
	700	4.3×10^{-8}	6.9×10^{-7}	5.1×10^{-3}	2.0×10^{-1}
	600	1.8×10^{-8}	1.9×10^{-7}	4.6×10^{-3}	9.0×10^{-2}
	500	1.1×10^{-10}	8.2×10^{-10}	8.3×10^{-5}	8.4×10^{-4}
	400	2.6×10^{-11}	4.6×10^{-11}	1.3×10^{-5}	2.6×10^{-5}
	300	1.4×10^{-12}	-	5.5×10^{-7}	-
Bare[1]	900	1.0×10^{-6}	3.0×10^{-5}	3.9×10^{-1}	11.3
	800	2.4×10^{-7}	9.9×10^{-6}	6.3×10^{-2}	4.8
	700	6.3×10^{-8}	7.2×10^{-7}	1.1×10^{-2}	2.7×10^{-1}
	600	1.1×10^{-8}	1.3×10^{-7}	3.9×10^{-3}	5.5×10^{-2}
	500	1.9×10^{-10}	1.1×10^{-9}	1.2×10^{-4}	6.0×10^{-4}
	400	3.5×10^{-11}	-	2.9×10^{-6}	-
	300	1.2×10^{-12}	-	1.7×10^{-7}	-
Prehydrided	600	9.1×10^{-9}	1.4×10^{-7}	3.5×10^{-3}	2.6×10^{-2}
	500	1.9×10^{-10}	1.2×10^{-9}	5.7×10^{-5}	7.0×10^{-4}
	400	4.1×10^{-12}	-	6.0×10^{-6}	-
	300	1.3×10^{-12}	-	7.3×10^{-7}	-
Prehydrided and steam preoxidized	600	1.1×10^{-8}	1.9×10^{-7}	6.8×10^{-4}	1.3×10^{-2}
	500	6.9×10^{-11}	1.3×10^{-9}	6.9×10^{-5}	5.1×10^{-4}
	400	1.3×10^{-11}	-	4.7×10^{-6}	-
	300	1.5×10^{-12}	-	6.2×10^{-7}	-

[1]Values from earlier work reported in NUREG/CR-6846.

50-200 wppm at 400 and 500°C, but the data are not sufficient to quantify this effect. We can state, based on the data in these figures, that the hydrogen concentration in Zirlo in the range of 100-1000 wppm has negligible deleterious effect on the kinetics of oxidation in air at temperatures in the range of 300-600°C. Figures 7.3 and 7.4 show rate constants for oxide growth as a function of hydrogen content in the alloy in the pre- and post-breakaway conditions, respectively. These data indicate negligible effect of hydrogen concentration in the range of 100-1000 wppm on the scale growth.

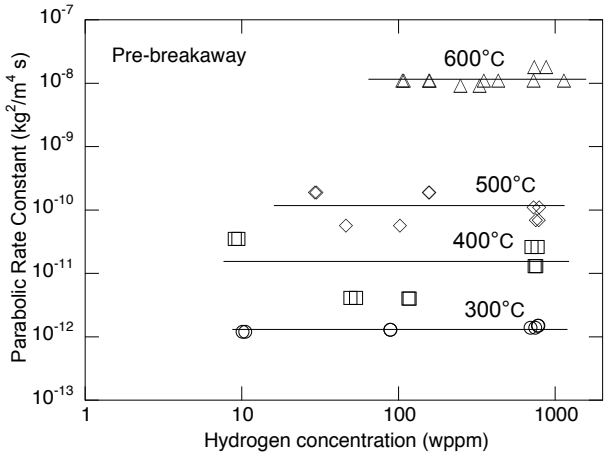

Figure 7.1. Parabolic rate constant in the pre-breakaway region for air oxidation of Zirlo, indicating minimal effect of hydrogen up to ≈1000 wppm on the oxidation kinetics at 300-600°C.

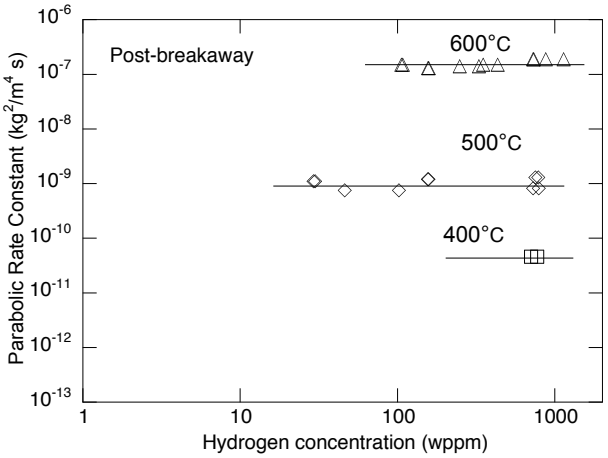

Figure 7.2. Parabolic rate constant in the post-breakaway region for air oxidation of Zirlo, indicating minimal effect of hydrogen up to ≈1000 wppm on the oxidation kinetics at 400-600°C.

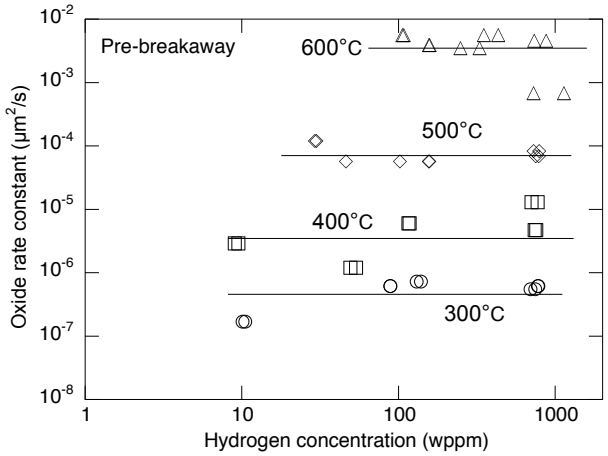

Figure 7.3. Oxide growthc rate constant in the pre-breakaway region for air oxidation of Zirlo, indicating minimal effect of hydrogen up to ≈1000 wppm on the scaling kinetics at 400-600°C.

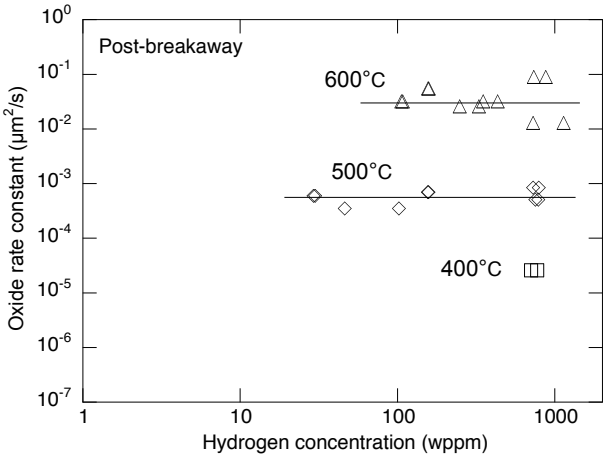

Figure 7.4. Oxide growth rate constant in the post-breakaway region for air oxidation of Zirlo, indicating minimal effect of hydrogen up to ≈1000 wppm on the scaling kinetics at 400-600°C.

8 Conclusion

An extensive study was conducted on unirradiated Zirlo alloy to establish the air oxidation kinetics in both prehydrided and prehydrided/steam-preoxidized conditions. Experimental data were obtained on the air oxidation kinetics of Zirlo cladding that had been prehydrided in hydrogen gas with or without steam preoxidation. Experiments were conducted in which Zirlo ring and capsule specimens were exposed in a hydrogen environment at 320°C and for various periods. Prehydriding treatment was tailored to obtain hydrogen concentrations in a range of 100-1000 wppm. Steam preoxidation treatment was conducted to obtain an oxide thickness of ≈25 μm. The prehydrided and prehydrided/steam-preoxidized Zirlo capsule specimens were subsequently oxidized in air at temperatures in the range of 300-600°C. The maximum air oxidation times ranged between ≈1000 h at 300°C and 300 h at 600°C. Weight-change and oxide-thickness data were developed at temperatures in the range of 300-600°C. The results were used to develop parabolic rate constants and oxide-growth rate constants. The following is a summary of the information developed from the test program:

- Hydrogen concentration in the specimens in the prehydrided condition was confined to a range of 100-1000 wppm.

- Extensive metallography of cross sections of prehydrided and air-oxidized specimens was conducted to measure the scale thickness and to establish the distribution of hydride precipitates across the cladding thickness.

- Hardness was measured on specimens with various treatments to examine the variation, if any, in the indentation size due to hydrogen ingress. Knoop hardness indentations were made at several locations across the cladding thickness in various specimens and exhibited negligible variation, which indicated an uniform distribution of hydrogen.

- The air-oxidized specimens with various pretreatments were analyzed for hydrogen content, and the results were used to correlate the parabolic oxidation rate and oxide-thickness growth rate with hydrogen concentration in the alloy.

- Data indicated that exposure of the Zirlo specimen at elevated temperature (e.g., steam preoxidation at 550°C) had a much more softening effect than the hardening effect that can result from higher hydrogen content (e.g., 695 and 735 wppm in steam-oxidized specimens).

- It is concluded that hydrogen concentrations in Zirlo in the range of 100-1000 wppm have negligible deleterious effect on the kinetics of oxidation in air at temperatures in the range of 300-600°C. Furthermore, the scaling data indicated negligible effect of hydrogen concentration in the range of 100-1000 wppm on the scale growth.

References

Com-Nougue, J., K. Omo, B. de Gelas, G. Beranger, and P. Lacombe, 1969, J. Less-Common Metals, 19, 259.

Cubiciotti, D., 1950, J. Am. Chem. Soc., 72, 4138.

Erickson, W. H. and D. Hardie, 1964, J. Nucl. Mat., 13, 254.

Gulbransen, E. A. and K. F. Andrew, 1957, Trans. Metall. Soc. AIME, 209, 394.

Gulbransen, E. A. and K. F. Andrew, 1955, Trans. AIME, 203, 136.

Hansen, M. and K. Anderko, 1958, Constitution of Binary Alloys, McGraw-Hill, 811.

Kearns, J. J., 1967, J. Nucl. Mat., 22, 292.

Kidson, G. V., 1966, Electrochem. Technol., 4, 193.

Leistikow, S. and H. v. Berg, 1987, "Investigation under Nuclear Safety Aspects of Zircaloy-4 Oxidation Kinetics at High Temperatures in Air," 2nd Workshop of German and Polish Research on High Temperature Corrosion of Metals, eds. W. J. Quadakkers, H. Schuster, and P. J. Ennis, Julich, Germany.

Leistikow, S., R. Kraft, and E. Pott, 1980, "The Interaction between Corrosion and Mechanical Stress at High Temperatures," Proc. Eur. Symp., Petten, p. 123.

Leistikow, S., G. Schanz, and H. V. Berg, 1978, "Kinetik und Morphologie der Isothermen Damf-Oxidation von Zircaloy-4 bei 700-1300°C," KfK 2587, Germany.

Mackay, T. L., 1963, Trans. Metall. Soc. AIME, 227, 1184.

Moalem, M. and D. R. Olander, 1991, "Oxidation of Zircaloy by Steam," J. Nucl. Mater., 182, 170.

Natesan, K. and W. K. Soppet, 2004, "Air Oxidation Kinetics for Zr-Based Alloys," Argonne National Laboratory Report ANL/03-32, NUREG/CR-6846.

Ostberg, G., 1962, J. Nucl. Mat., 5, 208.

Pawel, R. E., 1979, J. Electrochem. Soc., 126, 1111.

Pawel, R. E. and J. J. Campbell, 1980, J. Electrochem. Soc., 127, 2188.

Pemsler, J. P., 1962, J. Nucl. Mater., 7, 16.

Pemsler, J. P., 1964, J. Electrochem. Soc., 111, 1185.

Powers, D. A., L. N. Kmetyk, and R. C. Schmidt, 1994, "A Review of the Technical Issues of Air Ingression During Severe Reactor Accidents," Sandia National Laboratories, Albuquerque, NM, SAND94-0731.

Rosa, C. J., and W. W. Smeltzer, 1980, "The Oxidation of Zirconium in Oxygen/Nitrogen Atmospheres," Z. Metallkunde, p. 470.

Sawatzky, A., 1960, J. Nucl. Mat., 2, 62.

Wallwork, G. R., W. W. Smeltzer, and C. J. Rosa, 1964, Acta Metall., 12, 409.

Westerman, 1966, J. Nucl. Mat., 18, 31.

NRC FORM 335
(2–89)
NRCM 1102,
3201, 3202

U. S. NUCLEAR REGULATORY COMMISSION

BIBLIOGRAPHIC DATA SHEET

(See instructions on the reverse)

1. REPORT NUMBER
(Assigned by NRC. Add Vol., Supp., Rev., and Addendum Numbers, if any.)

NUREG/CR-6851
ANL-04/14

2. TITLE AND SUBTITLE

Hydrogen Effects on Air Oxidation of Zirlo Alloy

3. DATE REPORT PUBLISHED

MONTH	YEAR
September	2004

4. FIN OR GRANT NUMBER

Y6512

5. AUTHOR(S)

K. Natesan and W. K. Soppet

6. TYPE OF REPORT

Technical

7. PERIOD COVERED *(Inclusive Dates)*

8. PERFORMING ORGANIZATION – NAME AND ADDRESS *(If NRC, provide Division, Office or Region, U.S. Nuclear Regulatory Commission, and mailing address; if contractor, provide name and mailing address.)*

Argonne National Laboratory
9700 South Cass Avenue
Argonne, IL 60439

9. SPONSORING ORGANIZATION – NAME AND ADDRESS *(If NRC, type "Same as above": if contractor, provide NRC Division, Office or Region, U.S. Nuclear Regulatory Commission, and mailing address.)*

Division of Systems Analysis and Regulatory Effectiveness
Office of Nuclear Regulatory Research
U.S. Nuclear Regulatory Commission
Washington, DC 20555–0001

10. SUPPLEMENTARY NOTES

S. Basu, NRC Project Manager

11. ABSTRACT (200 words or less)

An experimental program was conducted to generate data on the air oxidation kinetics of unirradiated Zirlo cladding with preoxidation and prehydriding to simulate inventory of spent fuel discharge after a medium or high level of fuel burnup. The oxide layer on the cladding was formed by a preoxidation step in a steam environment for 140 h at 550°C, which resulted in an oxide thickness in the range of 25-30 μm. Prehydriding treatment was done by charging hydrogen to cladding and the process was tailored to produce hydrogen concentration in the range of 100-1000 wppm, typical of medium to high burnup cladding. The prehydrided and prehydrided/steam-preoxidized specimens were subsequently oxidized in air at temperatures in the range of 300-600°C. The maximum air oxidation times ranged between 300 h at 600°C and ≈1000 h at 300°C. Weight-change and oxide-thickness were measured on the specimens exposed at various times to establish the kinetics of the scaling process as a function of temperature. Extensive metallography and hardness measurements were performed on the tested specimens to examine the oxide scale development and hydrogen ingress into the material. Weight-change and oxide-thickness data, generated in the present program, were used to develop correlations to depict the air oxidation behavior of prehydrided alloys with and without steam preoxidation. A comparison of the oxidation data on Zirlo with and without prehydriding (performed in gas phase hydrogen and/or in steam) indicated that hydrogen concentration in the range of 100-1000 wppm had minimal effect on the Zirlo oxidation rate in air at temperatures in the range of 300-600°C.

12. KEY WORDS/DESCRIPTORS *(List words or phrases that will assist researchers in locating this report.)*

Air Oxidation
Hydrogen content
Oxide Thickness
Weight Change
Oxidation Correlations
Zirlo

13. AVAILABILITY STATEMENT

Unlimited

14. SECURITY CLASSIFICATION

(This Page)

Unclassified

(This Report)

Unclassified

15. NUMBER OF PAGES

16. PRICE

NRC FORM 335 (2–89)

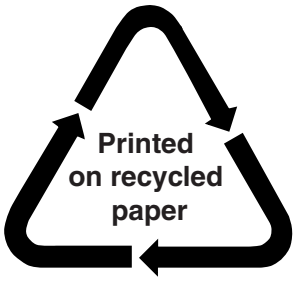

Federal Recycling Program